

# Matrix Models on Large Graphs

Mark Wexler<sup>†</sup>

*Department of Physics*

*Princeton University*

*Princeton, NJ 08544 USA*

We consider the spherical limit of multi-matrix models on regular target graphs, for instance single or multiple Potts models, or lattices of arbitrary dimension. We show, to all orders in the low temperature expansion, that when the degree of the target graph  $\Delta \rightarrow \infty$ , the free energy becomes independent of the target graph, up to simple transformations of the matter coupling constant. Furthermore, this universal free energy contains contributions only from those surfaces which are made up of “baby universes” glued together into trees, all non-universal and non-tree contributions being suppressed by inverse powers of  $\Delta$ . Each order of the free energy is put into a simple, algebraic form.

May 1993

---

<sup>†</sup> E-mail address: *wexler@puhep1.princeton.edu*

## 1. Introduction

Matrix models [1] are an efficient way to describe random surfaces, noncritical string theory, and perhaps other systems. A one-matrix model describes pure (i.e., not coupled to matter) surfaces and the bosonic string in zero dimensions. Its partition function is

$$\int D\phi e^{-\text{Tr}V(\phi)} \quad (1.1)$$

where  $\phi$  is an  $N \times N$  hermitian matrix, and  $V$  is some non-gaussian potential; in the remainder of this work, it will be chosen to be

$$V(\phi) = \frac{1}{2}\phi^2 + \frac{g}{\sqrt{N}}\phi^3. \quad (1.2)$$

Multi-matrix models describe random surfaces coupled to matter, or a string propagating in some target space. Their partition functions are of the form

$$\int D\phi_1 \cdots D\phi_\xi e^{-\text{Tr}(\sum_i V(\phi_i) - \frac{1}{2}\phi_i \Gamma_{ij} \phi_j)} \quad (1.3)$$

where the coupling matrix  $\Gamma$ , which depends on a matter coupling constant  $a$ , determines the matter model coupled to the surface, or the target space of the string. In this work, the free energy will always be defined in the spherical limit  $N \rightarrow \infty$ .

The matrix  $\Gamma$  may be thought of as the adjacency matrix of a labeled graph  $\mathcal{G}$ , which we shall call the *target graph*. One-matrix models have been solved exactly for a variety of potentials  $V(\phi)$  and for particular genera of the surface, as well as in the double scaling limit. Multi-matrix models have also been solved exactly, but only when the target graph  $\mathcal{G}$  is a tree, that is, when it has no cycles. This excludes a great many matter models (or target spaces), and in particular all those with central charge greater than one.

A method to deal with arbitrary target graphs has recently been proposed [2]: a low temperature expansion of the free energy, in powers of the matter coupling constant  $a$ . This reduces scalar multi-matrix model averages to contractions of tensor one-matrix model averages. Analogous to the low temperature expansion for ordinary lattice models, in  $n$ -th order one has some number of “blobs” which are open surfaces of uniform spin, connected by  $n$  edges which join blobs of unequal spin.

In the present work, we consider regular target graphs, *i.e.*, ones whose every vertex has the same degree or number of neighbors,  $\Delta$ . We show, *to all orders in the low temperature expansion*, that in the limit  $\Delta \rightarrow \infty$  the free energy of a multi-matrix model

becomes independent of its target graph and equal to some universal function,  $F_\infty$ , up to some simple transformations of  $a$ . Furthermore, we show that the only surfaces which contribute to the universal model are blobs joined into trees. Concretely, non-universal and non-tree terms in the free energy are suppressed by inverse powers of  $\Delta$ . Some examples of models having regular target graphs, which we treat in detail, are the  $q$ -state Potts model,  $d$ -dimensional lattice, and  $\nu$  copies of any regular model, where  $q, d$ , and  $\nu \rightarrow \infty$ . Finally, we derive a simple, closed expression for  $F_\infty$  in any order.

The  $d \rightarrow \infty$  limit of random surfaces has been discussed [3–4], in the context of the continuum  $d$ -dimensional model with Gaussian interaction for the embedding.<sup>1</sup> Both of these works argue that the worldsheet has a tree-like (or “branched polymer”) structure. Our results agree on this basic point. Beyond that, however, there are differences. Whereas we obtain entire open surfaces glued together into trees, according to [3–4] the Gaussian model is dominated in this limit by worldsheet tubes connected into trees. There is no contradiction, because the models are different. Indeed, it is encouraging that some kind of trees emerge in both models. Furthermore, the “branched polymers” of [3] appear at one of the critical regimes of our universal model (see last section): the critical point of the “matter”—it is to be remembered that the Gaussian model is always critical. The correspondence between our results and those of [3–4] leads one to suspect that our results are valid non-perturbatively (beyond the low temperature expansion).

This article is organized as follows. In the second section we summarize the old results on the low temperature expansion, and explain some new ones, in particular the explicit combinatorial rules for the diagrams in the partition function and in the free energy. In the third section we prove the assertions concerning universality and trees, and derive the exact form of  $F_\infty$ , which involves a sum over labeled trees. In the fourth section we go through some combinatorial manipulations to put each term in the sum into an algebraic form. In the final section, we discuss some of the implications of these results, including the critical behavior of the universal model, and suggest directions for further work.

## 2. The low temperature expansion

### 2.1. The target graph

If the matrix model represents a bosonic string, the target graph  $\mathcal{G}$  is the discrete target space of the string, its edges the “metric.” For instance, it might be reasonable

---

<sup>1</sup> To be contrasted with the Feynman propagators of the  $\mathcal{L}_d$  model considered here

to take  $\mathcal{G} = \mathcal{L}_d$ , the infinite  $d$ -dimensional hypercubic lattice with periodic boundary conditions whose central charge is  $d$ . If the matrix model represents a random surface, the vertices of the target graph are the states of the matter, and the (weighted) edges are the interactions between the states.<sup>2</sup> For example, if the matter is a  $q$ -state Potts model,  $\mathcal{G}$  is  $\mathcal{K}_q$ , the complete graph on  $q$  vertices. The central charge is  $0, \frac{1}{2}, \frac{4}{5}$ , and  $1$  for  $q = 1, 2, 3$ , and  $4$ , and undefined for  $q > 4$  where KPZ scaling breaks down. So far, all edges of the target graph have the same weight,  $a$ . In either case, we shall use the word “spin” to designate the value of the vertex of  $\mathcal{G}$  assigned to each plaquette of the surface.

In the case of a random surface with matter, one might also consider multiple “uncoupled” matter models [5]. For instance,  $\nu$  species of, say, Potts models live on each elementary polygon of the surface, each spin interacting with nearest neighbor spins of the *same* species only. On a fixed surface this would be trivial: the partition function would just factorize. On a random surface, however, the different species effectively interact with each other because each interacts with the surface. The central charge of a multiple model is the sum of the individual central charges; the coupling matrix  $\Gamma$  is the direct product of the individual coupling matrices. As a result, the edges of the target graph of a multiple model never have uniform weights. For  $\nu$  Ising models, for example, the vertices of  $\mathcal{G}$  are those of a  $\nu$ -dimensional hypercube, labeled  $0, 1, \dots, 2^\nu - 1$ , but each vertex is connected to every other; any two vertices are connected with the weight  $a^\delta$ , where  $\delta$  is the number of digits by which the binary representations of the labels of the two vertices differ. We shall call this target graph  $\mathcal{Q}_\nu$ .

It should be noted that all target graphs mentioned above are regular. The degree  $\Delta = d$  and  $q - 1$  for the lattice and Potts model, respectively. For multiple models, we define  $\Delta$  to be the degree of  $\tilde{\mathcal{G}}$ , the graph  $\mathcal{G}$  with all  $a^2, a^3$ , etc. edges removed; for  $\nu$  Ising models, therefore,  $\tilde{\mathcal{G}}$  is the ordinary  $d$ -dimensional hypercube and  $\Delta = \nu$ . In general, for  $\nu$  copies of a single model with degree  $\delta$ ,  $\Delta = \nu\delta$ . In this work, we shall treat only regular target graphs, although one would get similar results if this condition were to be somewhat relaxed.

---

<sup>2</sup> Strictly speaking, the “target graph” here should have adjacency matrix  $(1 - \Gamma)^{-1}$ , the matter propagator. For the types of matter which we consider here—(multiple) Potts models—the two are equivalent up to a rescaling of the matrix fields and a transformation  $a \rightarrow -f(a)$ , where  $f$  is a monotonically increasing function in the relevant interval, and  $f(a) \approx a$  when  $a \ll 1$ .

## 2.2. The partition function

For a particular target graph  $\mathcal{G}$  with  $\xi$  vertices, the partition function of the matrix model is defined

$$Z_{\mathcal{G}}(g, a) = \frac{\int D\mu(\phi_1) \cdots D\mu(\phi_{\xi}) e^{\frac{1}{2} \text{Tr} \phi_i \Gamma_{ij} \phi_j}}{D\mu(\phi_1) \cdots D\mu(\phi_{\xi})} \equiv \left\langle e^{\frac{1}{2} \text{Tr} \phi_i \Gamma_{ij} \phi_j} \right\rangle \quad (2.1)$$

$$D\mu(\phi) \equiv D\phi e^{-\text{Tr} V(\phi)}$$

The coupling matrix  $\Gamma$  depends on the matter coupling constant  $a$  ( $a = e^{-\beta}$ , where  $\beta$  is the inverse of the matter temperature). We wish to expand the partition function in powers of  $a$ :

$$Z_{\mathcal{G}}(g, a) = 1 + \sum_{n=1}^{\infty} \frac{z_n}{n!} a^n \quad (2.2)$$

For single models—where all edges of  $\mathcal{G}$  are weighted 0 or  $a$ —the  $n$ -th order coefficient  $z_n$  is a sum of possible terms of the form  $\langle \text{Tr} \phi_{i_1} \phi_{j_1} \cdots \text{Tr} \phi_{i_n} \phi_{j_n} \rangle$ , where some of the indices may be equal. For a multiple model, in  $n$ -th order one has a sum of terms  $\langle \text{Tr} \phi_{i_1} \phi_{j_1} \cdots \text{Tr} \phi_{i_m} \phi_{j_m} \rangle$  where  $m \leq n$  and

$$\prod_{k=1}^m G_{i_k j_k} = a^m. \quad (2.3)$$

Each term  $\langle \text{Tr} \phi_i \phi_j \cdots \rangle$  may be thought of as a subgraph  $\mathcal{H} \subseteq \mathcal{G}$ : the vertices of  $\mathcal{H}$  are a subset of those of  $\mathcal{G}$ , and the edges likewise, except that  $\mathcal{H}$  is allowed to have multiple edges. Each factor  $\text{Tr} \phi_i \phi_j$  gives an edge in  $\mathcal{H}$  between vertices  $i$  and  $j$ . Many subgraphs are isomorphic and therefore equal, for example  $\langle \text{Tr} \phi_1 \phi_2 \rangle$  and  $\langle \text{Tr} \phi_2 \phi_3 \rangle$ . We shall therefore take the subgraphs  $\mathcal{H}$  to have unlabeled edges and vertices, because it is much more efficient; but in counting them, we shall remember that their *edges* are labeled.

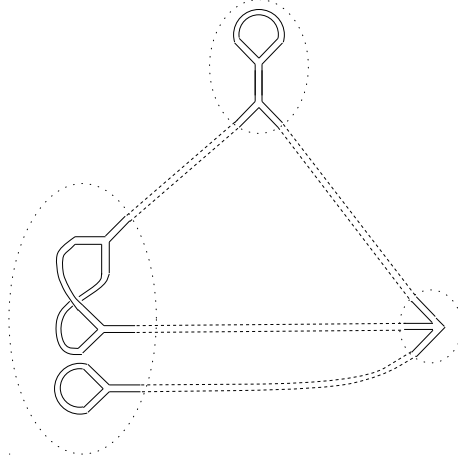
Consider, for instance, the term  $\langle \text{Tr} \phi_1 \phi_2 (\text{Tr} \phi_2 \phi_3)^2 \text{Tr} \phi_3 \phi_1 \rangle$ , which might arise in fourth or higher order in the partition function. Its corresponding (unlabeled) graph  $\mathcal{H}$  is



The coefficient multiplying this term counts the number of ways in which the graph  $\mathcal{H}$ , with labeled edges, may be embedded in  $\mathcal{G}$ . In the  $q$ -state Potts model ( $\mathcal{G} = \mathcal{K}_q$ ),  $\mathcal{H}$  occurs

only in  $z_4$  with the coefficient  $\frac{1}{2}q(q-1)^2$ ; in  $\nu$  Ising models ( $\mathcal{G} = \mathcal{Q}_\nu$ ), with the coefficient  $2^{\nu-1}\nu^2(\nu-1)$  in  $z_5$  and with other coefficients in higher orders; and  $\mathcal{H}$  does not occur in the lattice  $\mathcal{L}_d$ .

The interpretation in terms of surfaces is as follows: each vertex of a subgraph  $\mathcal{H}$  is an open surface, a “blob.” All spins on this blob are equal, or “frozen” at the same value, and therefore the surface can be described by a pure gravity matrix model (see below). Spins on two neighboring blobs are unequal. It should be noted that a blob contains contributions from both connected and disconnected surfaces. For instance, one of the graphs<sup>3</sup> which contribute to (2.4) is



Each blob has many internal edges which connect equal spins. There are only four edges (“bridges,” dotted in the drawing) which connect blobs of unequal spin. We shall call the subgraphs  $\mathcal{H}$  “Z-skeletons”; the meat on each vertex of a Z-skeleton is a blob, an open surface with uniform spin.

As a concrete example, we give the low temperature expansions of the partition functions to third order for three different models. The Z-skeletons are represented graphically,

---

<sup>3</sup> We use the words “graph” and “surface” interchangeably for two objects that are dual to one another.

as above. First, the partition function of the  $q$ -state Potts model,  $\mathcal{G} = \mathcal{K}_q$ :

$$\begin{aligned}
Z = & 1 + \binom{q}{2} \bullet \text{---} \bullet a \\
& + \frac{1}{2} \left[ \binom{q}{2} \bullet \text{---} \bullet \text{---} \bullet + 6 \binom{q}{3} \bullet \text{---} \bullet \text{---} \bullet + 6 \binom{q}{4} \bullet \text{---} \bullet \text{---} \bullet \right] a^2 \\
& + \frac{1}{6} \left[ \binom{q}{2} \bullet \text{---} \bullet \text{---} \bullet + 24 \binom{q}{4} \bullet \text{---} \bullet \text{---} \bullet + 72 \binom{q}{4} \bullet \text{---} \bullet \text{---} \bullet + 6 \binom{q}{3} \triangle \right. \\
& \quad + 18 \binom{q}{3} \bullet \text{---} \bullet \text{---} \bullet + 180 \binom{q}{5} \bullet \text{---} \bullet \text{---} \bullet + 18 \binom{q}{4} \bullet \text{---} \bullet \text{---} \bullet \\
& \quad \left. + \left( \binom{q}{2}^3 - \frac{q}{4}(q-1)(6q^3 - 35q^2 + 77q - 60) \right) \bullet \text{---} \bullet \text{---} \bullet \right] a^3 \\
& + \mathcal{O}(a^4)
\end{aligned} \tag{2.5}$$

Now a  $d$ -dimensional hypercubic lattice,  $\mathcal{G} = \mathcal{L}_d$  with length  $L$  (which will drop out later in the calculations) and periodic boundary conditions ( $\ell \equiv dL^d$ ):

$$\begin{aligned}
Z = & 1 + \ell \bullet \text{---} \bullet a \\
& + \frac{1}{2} \left[ \ell \bullet \text{---} \bullet \text{---} \bullet + 2(2d-1)\ell \bullet \text{---} \bullet \text{---} \bullet + (\ell - 4d + 1)\ell \bullet \text{---} \bullet \text{---} \bullet \right] a^2 \\
& + \frac{1}{6} \left[ \ell \bullet \text{---} \bullet \text{---} \bullet + 2(2d-1)(2d-2)\ell \bullet \text{---} \bullet \text{---} \bullet + 6(2d-1)^2 \ell \bullet \text{---} \bullet \text{---} \bullet \right. \\
& \quad + 6(2d-1)\ell \bullet \text{---} \bullet \text{---} \bullet + 6(2d-1)(\ell - 6d + 2)\ell \bullet \text{---} \bullet \text{---} \bullet + 3(\ell - 4d + 1)\ell \bullet \text{---} \bullet \text{---} \bullet \\
& \quad \left. + (\ell^2 - 12d\ell + 3\ell + 40d^2 - 24d + 4)\ell \bullet \text{---} \bullet \text{---} \bullet \right] a^3 \\
& + \mathcal{O}(a^4)
\end{aligned} \tag{2.6}$$

Finally, a multiple model:  $\nu$  Ising models,  $\mathcal{G} = \mathcal{Q}_\nu$ :

$$\begin{aligned}
Z &= 1 + \frac{\nu}{2} 2^\nu \bullet \text{---} a \\
&+ \frac{1}{2} \left[ \frac{\nu}{2} \bullet \text{---} \bullet + 2\nu(\nu-1) \bullet \text{---} \bullet \text{---} \bullet + \frac{\nu}{2} (\frac{\nu}{2} 2^\nu - 2\nu + 1) \begin{array}{c} \bullet \text{---} \bullet \\ \bullet \text{---} \bullet \end{array} + \frac{\nu}{2} (\nu-1) \bullet \text{---} \bullet \right] 2^\nu a^2 \\
&+ \frac{1}{6} \left[ \frac{\nu}{2} \bullet \text{---} \bullet + \nu(\nu-1)(\nu-2) \begin{array}{c} \bullet \\ \bullet \text{---} \bullet \\ \bullet \end{array} + 3\nu(\nu-1)^2 \bullet \text{---} \bullet \text{---} \bullet + 3\nu(\nu-1) \bullet \text{---} \bullet \right] \\
&\quad \frac{3\nu}{2} (\nu-1)(2^\nu \nu - 6\nu + 4) \begin{array}{c} \bullet \text{---} \bullet \\ \bullet \text{---} \bullet \end{array} + \frac{3\nu}{4} (\nu-1)(2^\nu \nu - 4\nu + 2) \begin{array}{c} \bullet \text{---} \bullet \\ \bullet \text{---} \bullet \end{array} \\
&\quad + \frac{\nu}{8} (2^{2\nu} \nu^2 - 122^\nu \nu^2 + 62^\nu \nu + 40\nu^2 - 48\nu + 16) \begin{array}{c} \bullet \text{---} \bullet \\ \bullet \text{---} \bullet \\ \bullet \text{---} \bullet \end{array} \\
&\quad + 3\nu^2 (\nu-1) \bullet \text{---} \bullet \text{---} \bullet + \frac{3\nu^2}{4} (\nu-1)(2^\nu - 4) \begin{array}{c} \bullet \text{---} \bullet \\ \bullet \text{---} \bullet \end{array} + \frac{\nu}{2} (\nu-1)(\nu-2) \bullet \text{---} \bullet \Big] a^3 \\
&+ \mathcal{O}(a^4)
\end{aligned} \tag{2.7}$$

### 2.3. Calculating the blobs

How can we calculate the contribution of each Z-skeleton to the partition function? This can be done by expressing multi-matrix averages of traces in terms of matrix components, so that they can be decomposed into contractions of one-matrix tensor averages. For example, our friend  $\langle \text{Tr} \phi_1 \phi_2 (\text{Tr} \phi_2 \phi_3)^2 \text{Tr} \phi_3 \phi_1 \rangle$  can be decomposed into

$$\langle \phi_\beta^\alpha \phi_\delta^\gamma \rangle \langle \phi_\alpha^\beta \phi_\zeta^\epsilon \phi_\theta^\eta \rangle \langle \phi_\epsilon^\zeta \phi_\eta^\theta \phi_\gamma^\delta \rangle \tag{2.8}$$

In the latter expression, the averages are with respect to a “pure gravity” one-matrix model:  $\langle \mathcal{O} \rangle \equiv \int D\mu(\phi) \mathcal{O}(\phi) / \int D\mu(\phi)$ . The three tensors in this expressions are just the three blobs of the Z-skeleton  $\triangleleft$ . Thus each blob with  $\delta$  adjoining bridges is a rank  $(\delta, \delta)$  tensor, and each bridge contracts an upper and a lower index.<sup>4</sup>

The task is to calculate the one-matrix model vertex factor arising from a  $\delta$ -valent blob:

$$B_{\beta_1 \dots \beta_\delta}^{\alpha_1 \dots \alpha_\delta} \equiv \langle \phi_{\beta_1}^{\alpha_1} \dots \phi_{\beta_\delta}^{\alpha_\delta} \rangle \tag{2.9}$$

---

<sup>4</sup> It is necessary to distinguish between upper and lower indices to preserve the symmetry under unitary transformations.



A convenient way to do this is to contract (2.9) with  $\Lambda_{\beta_1}^{\alpha_1} \cdots \Lambda_{\beta_\delta}^{\alpha_\delta}$ , where  $\Lambda$  is some  $N \times N$  hermitian matrix. Then the right-hand side of (2.9) becomes  $\langle (\text{Tr } \Lambda \phi)^\delta \rangle$ , for which the generating functional is the external field integral

$$Q(\Lambda, g) = \int D\mu(\phi) e^{\sqrt{N} \text{Tr } \Lambda \phi} \quad (2.10)$$

$P = \frac{1}{N^2} \log Q$  has been explicitly calculated in the spherical limit for an arbitrary matrix  $\Lambda$  by Kazakov and Kostov [6] and by Gross and Newman [7]. See [2] for a summary of the result, as well as for explicit details of the vertex factor calculation.

To understand the expansion of  $Q$  in powers of  $\Lambda$ , we put  $\Lambda \rightarrow \epsilon \Lambda$  and expand  $P$ :

$$P = p_0 - p_1 \epsilon + \frac{1}{2} p_2 \epsilon^2 - \frac{1}{6} p_3 \epsilon^3 + \cdots \quad (2.11)$$

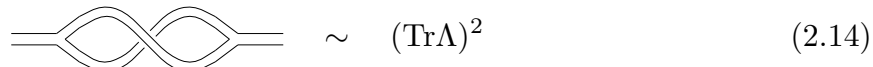
The first few terms are:

$$\begin{aligned} p_1 &= N^{-1} \text{Tr } \Lambda (3g + 108g^3 + 7776g^5 + \cdots) \\ &\equiv N^{-1} \text{Tr } \Lambda p_{1,1} \\ p_2 &= N^{-1} \text{Tr } \Lambda^2 (27g^2 + 1944g^4 + \cdots) \\ &\quad + N^{-2} (\text{Tr } \Lambda)^2 (9g^2 + 1296g^4 + \cdots) \\ &\equiv N^{-1} \text{Tr } \Lambda^2 p_{2,1} + N^{-2} (\text{Tr } \Lambda)^2 p_{2,2} \\ p_3 &= N^{-1} \text{Tr } \Lambda^3 (6g + 540g^3 + 58320g^5 + \cdots) \\ &\quad + N^{-2} \text{Tr } \Lambda \text{Tr } \Lambda^2 (324g^3 + 69984g^5 + \cdots) \\ &\quad + N^{-3} (\text{Tr } \Lambda)^3 (7776g^5 + \cdots) \\ &\equiv N^{-1} \text{Tr } \Lambda^3 p_{3,1} + N^{-2} \text{Tr } \Lambda \text{Tr } \Lambda^2 p_{3,2} + N^{-3} (\text{Tr } \Lambda)^3 p_{3,3} \end{aligned} \quad (2.12)$$

We observe that  $p_{n,1}/(n-1)!$ , the coefficient of  $N \text{Tr } \Lambda^n$  in  $p_n$  is just the connected  $n$ -point Green's function of the cubic one-matrix model [8], which is as it should be. What, then, are the other terms which occur:  $p_{n,2}$ , etc.? The matrix  $\Lambda$  is attached to the external vertices, so one way to get, say,  $(\text{Tr } \Lambda)^2$  is through a disconnected two-point function. But we know that  $P$  must be connected. The only other possibility is to have *twisted* graphs. For instance, a typical graph in  $p_{2,1}$  is

$$\begin{array}{c} \text{---} \text{---} \text{---} \\ \text{---} \text{---} \text{---} \\ \text{---} \text{---} \text{---} \end{array} \sim \text{Tr } \Lambda^2 \quad (2.13)$$

while a typical graph in  $p_{2,2}$  is

$$
(2.14)$$

Both of these graphs are “spherical,” because by attaching tadpole endcaps to the external lines one obtains closed spherical graphs. But by tracing the indices in graph (2.14), one finds that the two  $\Lambda$ ’s never connect, giving the factor  $(\text{Tr}\Lambda)^2$ . The same holds for all  $p_{n,\tau>1}$ : the surfaces which contribute to them can be transformed into ordinary connected Green’s functions by untwisting the ends.

The  $n$ -th order term in  $Q$  has the same contributions as its counterpart in  $P$ , the twisted and untwisted connected graphs. It also has, of course, twisted and untwisted disconnected graphs.

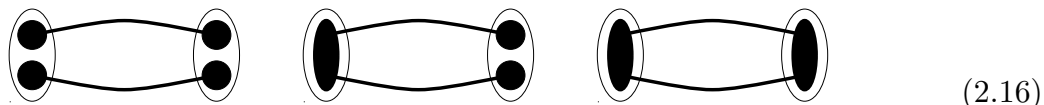
#### 2.4. The free energy

The partition function looks rather complicated: it contains connected and disconnected  $Z$ -skeletons, which contain connected and disconnected, twisted and untwisted blobs. If some of the blobs are disconnected, the whole graph may still be connected; but if the  $Z$ -skeleton is disconnected, the graph will be as well. Things are simplified immensely when one takes the logarithm to calculate the free energy

$$\begin{aligned}
 F_{\mathcal{G}}(g, a) &= \frac{1}{\xi N^2} \log \frac{Z_{\mathcal{G}}(g, a)}{Z_{\mathcal{G}}(g, 0)} \\
 &= f_1 a + \frac{1}{2} f_2 a^2 + \frac{1}{6} f_3 a^3 + \dots
 \end{aligned}
 \tag{2.15}$$

(we recall that  $\xi$  is the number of vertices (“volume”) in the target graph  $\mathcal{G}$ ). We can further simplify the calculations by expressing everything in terms of the coefficients  $p_{m,\tau}$  in the connected generating functional  $P(\Lambda)$ , rather than those in the actual disconnected blob-generating functional  $Q(\Lambda)$ .

When passing from the partition function to the free energy, one is of course left with only the connected graphs. Another major change occurs in the quality of the skeletons. Consider, for instance, one Ising model, whose target graph  $\mathcal{G} = \mathcal{Q}_1 = \bullet \text{---} \bullet$ . The  $Z$ -skeleton  $\bullet \text{---} \bullet$  does not occur in any order, because it is impossible to embed it in  $\mathcal{G}$ . The  $Z$ -skeleton  $\bullet \text{---} \bullet$  however does occur in second order. Its bivalent blobs may be connected or disconnected, which gives rise to the following possibilities:

$$
(2.16)$$

The first of these is disconnected, so it gets canceled. The last is the skeleton  $\bullet \rightleftharpoons \bullet$ . The skeleton in the middle, however, is the graph  $\bullet \text{---} \bullet$ , which does not occur as a Z-skeleton. When we express everything in terms of connected blobs rather than the “natural blobs” which were first encountered, we find that many new skeletons are allowed in addition to the Z-skeletons, and that the combinatorial rules for finding the coefficients of the skeletons in the free energy are of course different as well. We shall call these new skeletons “F-skeletons.”

First, consider single models. As a concrete example, here is the free energy to third order of the  $q$ -state Potts model:

$$\begin{aligned}
F = & \frac{1}{2}(q-1)\tilde{p}_1^2 a + \left[ \frac{1}{2}(q-1)^2 \tilde{p}_1^2 \tilde{p}_2 + \frac{1}{4} p_{2,1}^2 \right] a^2 + \\
& + \left[ \frac{1}{2}(q-1)^3 \tilde{p}_1^2 \tilde{p}_2^2 + \frac{1}{6}(q-1)^3 \tilde{p}_1^3 \tilde{p}_3 + \frac{1}{6}(q-1)(q-2) p_{2,2}^3 \right. \\
& \left. + \frac{1}{2}(q-1)^2 \tilde{p}_1 p_{2,1} p_{3,1} + \frac{1}{6}(q-1)^2 \tilde{p}_1 p_{2,1} p_{3,2} + \frac{1}{24}(q-1) p_{3,1}^2 \right] a^3 + \mathcal{O}(a^4)
\end{aligned} \tag{2.17}$$

and of the  $d$ -dimensional lattice ( $D \equiv 2d$ ):

$$\begin{aligned}
F = & \frac{1}{2} D \tilde{p}_1^2 a + \left( \frac{1}{2} D^2 \tilde{p}_1^2 \tilde{p}_2 + \frac{1}{4} D p_{2,1}^2 \right) a^2 + \\
& + \left( \frac{1}{2} D^3 \tilde{p}_1^2 \tilde{p}_2^2 + \frac{1}{6} D^3 \tilde{p}_1^3 \tilde{p}_3 + \frac{1}{2} D^2 \tilde{p}_1 p_{2,1} p_{3,1} + \frac{1}{6} D^2 \tilde{p}_1 p_{2,1} p_{3,2} + \frac{1}{24} D p_{3,1}^2 \right) a^3 + \mathcal{O}(a^4)
\end{aligned} \tag{2.18}$$

where  $\tilde{p}_n = \sum_{\tau} p_{n,\tau}$ . We would like to identify the above terms with F-skeletons. This is not hard, because a factor  $p_{n,\tau}^k$  means that there are  $k$   $n$ -valent vertices in the F-skeleton;  $\tau - 1$  is the number of twists of the corresponding blob. This “degree sequence” uniquely identifies small graphs, so that we can make the following dictionary (omitting the twist index):

$$\begin{array}{cccc}
p_1^2 \rightarrow \bullet \text{---} \bullet & p_1^2 p_2 \rightarrow \bullet \text{---} \bullet \text{---} \bullet & p_2^2 \rightarrow \bullet \rightleftharpoons \bullet & p_1^2 p_2^2 \rightarrow \bullet \text{---} \bullet \text{---} \bullet \\
p_1^3 p_3 \rightarrow \begin{array}{c} \bullet \\ | \\ \bullet \text{---} \bullet \end{array} & p_2^3 \rightarrow \triangle & p_1 p_2 p_3 \rightarrow \bullet \rightleftharpoons \bullet \text{---} \bullet & p_3^2 \rightarrow \bullet \rightleftharpoons \bullet
\end{array}$$

We are now ready to give the “Feynman rules” for the F-skeletons of single models. The F-skeletons  $\mathcal{H}$  are no longer subgraphs of the target graph  $\mathcal{G}$ , as we showed above. Instead, the vertices of  $\mathcal{G}$  are to be thought of as “colors” with which the vertices of  $\mathcal{H}$  are colored—the ordinary notion of spin. Two adjacent vertices of  $\mathcal{H}$  must have different

colors, and these two colors must be adjacent in  $\mathcal{G}$ . Thus the target graph  $\mathcal{G}$  provides both the possible colors for the F-skeletons, as well as the rules on how the colors may be combined.

For a particular  $\mathcal{G}$ , a graph  $\mathcal{H}$  may appear as an F-skeleton provided that the latter may be colored according to the rules of the former. Consider some particular such unlabeled graph  $\mathcal{H}$  with  $n$  edges, and which therefore appears in the  $n$ -th order term  $f_n$ . The coefficient of  $\mathcal{H}$  in  $f_n$  is a product of

- the number of distinct ways to label the edges of  $\mathcal{H}$ , which is  $n!$  divided by the order of the automorphism group of  $\mathcal{H}$ ;
- and a factor  $C_{\mathcal{G}}(\mathcal{H})$ , the number of ways to color each *labeled* version of  $\mathcal{H}$ .

Since  $f_n$  appears in the free energy divided by  $n!$ , and the free energy is divided by  $\xi$  (the volume of  $\mathcal{G}$ ), the total factor of  $\mathcal{H}$  in the free energy is

$$\frac{C_{\mathcal{G}}(\mathcal{H})}{\xi |\text{Aut}(\mathcal{H})|}. \quad (2.19)$$

However, an F-skeleton  $\mathcal{H}$  is represented in the free energy by more than one combination of the vertex factors  $p_{n,\tau}$  because the blobs may be twisted in different ways. For example,  $\circ \rightleftarrows \bullet$  may be represented by  $\tilde{p}_1 p_{2,1} p_{3,1}$  or by  $\tilde{p}_1 p_{2,2} p_{3,2}$ , among others. Each of these combinations may have a different coefficient, for which the expression (2.19) is an *upper bound*. The reason is topological: the whole graph must be spherical, while certain contractions of twisted blobs may yield non-spherical graphs. If one takes the untwisted  $n$ -valent vertex factors  $p_{n,1}$  for all vertices, one obtains the largest possible coefficient, which may still be less than the bound (2.19).<sup>5</sup> To illustrate for the F-skeleton  $\circ \rightleftarrows \bullet$  in (2.17) and (2.18): the upper bound given by (2.19) is  $\frac{1}{2}(q-1)^2$ ; this is saturated by  $\tilde{p}_1 p_{2,1} p_{3,1}$ ;  $\tilde{p}_1 p_{2,1} p_{3,2}$  is suppressed to  $\frac{1}{6}(q-1)^2$ ; the other four combinations are completely suppressed.

The free energy rules are similar for multiple models, except that in order  $n$  there are F-skeletons with  $n$  and fewer edges, as there are edges in  $\mathcal{G}$  weighted  $a^2$ ,  $a^3$ , etc. For  $\nu$  Ising models ( $\mathcal{G} = \mathcal{Q}_\nu$ ), the free energy to third order is

$$\begin{aligned} F = & \frac{1}{2} \nu \tilde{p}_1^2 a + \\ & + \left[ \frac{1}{2} \nu^2 \tilde{p}_1^2 \tilde{p}_2 - \frac{1}{4} \nu p_{2,1}^2 + \frac{1}{4} \nu(\nu+1) \tilde{p}_1^2 \right] a^2 + \\ & + \left[ \frac{1}{2} \nu^3 \tilde{p}_1^2 \tilde{p}_2^2 + \frac{1}{6} \nu^3 \tilde{p}_1^3 \tilde{p}_3 + \frac{1}{2} \nu^2 \tilde{p}_1 p_{2,1} p_{3,1} + \frac{1}{6} \nu^2 \tilde{p}_1 p_{2,1} p_{3,2} + \frac{1}{24} \nu p_{3,1}^2 + \right. \\ & \left. + \frac{1}{2} \nu^2 (\nu-1) \tilde{p}_1^2 \tilde{p}_2 + \frac{1}{12} \nu(\nu-1)(\nu-2) \tilde{p}_1^2 \right] a^3 + \mathcal{O}(a^4) \end{aligned} \quad (2.20)$$

---

<sup>5</sup> This occurs for F-skeletons with cycles or multiple edges; see below.

For  $\nu = 1$  this can be checked [2] against the exact solution for one Ising model with cubic vertices [9]. One uses the same dictionary as before to translate from symbols to graphs. In each order  $n$ , the graphs with  $n$  edges follow the same combinatorial rules as single models. (To be more precise, the rules that would obtain for target graph  $\tilde{\mathcal{G}}$ , the graph  $\mathcal{G}$  with all  $a^2, a^3$ , etc. edges deleted. In the case  $\mathcal{G} = \mathcal{Q}_\nu$ ,  $\tilde{\mathcal{G}}$  is the ordinary  $\nu$ -dimensional hypercube.) The graphs with fewer than  $n$  edges have modified coefficients, due to

- a modified coloring factor  $C_{\mathcal{G}}(\mathcal{H}, n)$  (given a vertex of  $\mathcal{Q}_\nu$ , for example, there are  $\nu$  other vertices reachable by edges weighted  $a$ ,  $\binom{\nu}{2}$  vertices reachable by  $a^2$ -edges, and so on);
- an “weight-entropy” factor which counts the number of ways that the weights of the edges can be chosen so that their weights satisfy (2.3).

In a multiple model, once an F-skeleton appears in  $n$ -th order, it appears in all higher orders as well. The combinatorics of multiple models will be discussed in greater detail below.

### 3. Large target graphs

On examining the expansions (2.17), (2.18), and (2.20) for the free energy of three different models, one notices some patterns:

- the  $n$ -th order term  $f_n$  is a degree  $n$  polynomial in  $\Delta$ , the degree of  $\mathcal{G}$  or  $\tilde{\mathcal{G}}$ ;
- the coefficient of  $\Delta^n c^n$  in the free energy—which we shall call  $h_n$ —contains contributions only from those F-skeletons which are trees;<sup>6</sup>
- for the single models (2.17) and (2.18), the leading coefficients  $h_n$  are, in fact, identical; the  $h_n$  of the multiple model (2.20) are equal to the above if one ignores all F-skeletons with fewer than  $n$  edges;
- the coefficients of the trees do not care about the twists of the blobs; in other words, the vertex factors  $p_{n,\tau}$  in the tree coefficients always occur as the sums  $\tilde{p}_n$ .

These patterns are, in fact, not coincidental, and can easily be shown to hold for all regular target graphs  $\mathcal{G}$ , and to all orders  $n$  in the low temperature expansion. Because of assertion (a) (see below), when  $\Delta \rightarrow \infty$  we can ignore all terms in order  $n$  but  $h_n$ . Here we demonstrate the above assertions, and in the next section we derive simple expressions for  $h_n$ .

---

<sup>6</sup> This is reminiscent of, but not identical to, the result of Erdős and Rényi [10] that finite random subgraphs of  $\mathcal{K}_n$  for  $n \rightarrow \infty$  are almost always forests of trees.

The number of ways to label the edges of an F-skeleton  $\mathcal{H}$  (which has  $v$  vertices) depends only on  $\mathcal{H}$  and not on the target graph  $\mathcal{G}$ . For single models, the entire dependence of the coefficient of  $\mathcal{H}$  on  $\mathcal{G}$  is contained in the coloring factor  $C_{\mathcal{G}}(\mathcal{H})$ ; for multiple models, the dependence on  $\mathcal{G}$  is in the modified coloring factor  $C_{\mathcal{G}}(\mathcal{H}, n)$ . It is easy to see that  $C_{\mathcal{G}}(\mathcal{H})$  has the upper bound

$$C_{\mathcal{G}}(\mathcal{H}) \leq \xi \Delta^{v-1}, \quad (3.1)$$

which can be shown by picking an arbitrary vertex of  $\mathcal{H}$  that can be colored  $\xi$  different ways, and thereafter traveling to every other vertex of  $\mathcal{H}$ , noticing that when one moves from a colored to a yet-to-be-colored vertex, one has at most  $\Delta$  new colors to choose from. By induction, trees saturate the bound (3.1). The argument is analogous for multiple models. One has  $\xi$  colors for the first vertex of  $\mathcal{H}$ , and for each subsequent vertex, traveling along an  $a^k$ -edge of  $\mathcal{G}$ , one has at most  $\binom{\Delta}{k} \leq \Delta^k$  colors to choose from; using (2.3), we obtain the same bound (3.1). This demonstrates assertion (a).

By “tree,” we mean an F-skeleton which contains neither cycles nor multiple edges. Assertion (b) is now trivial, following from the upper bound (3.1) and the fact that a tree with  $n$  edges always has  $n + 1$  vertices, while a connected non-tree graph with  $n$  edges always has  $n$  or fewer vertices.

Having proved (b), we can ignore all graphs but trees when calculating  $h_n$ . Since trees saturate the bound (3.1), their coloring factors are asymptotically (for single models)

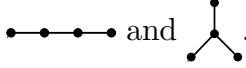
$$\frac{C_{\mathcal{G}}(\mathcal{H})}{\xi} = \Delta^{|\mathcal{H}|} + \mathcal{O}(\Delta^{|\mathcal{H}|-1}) \quad (3.2)$$

Because the coefficient of leading term is unity, the *maximum* contribution of a tree  $\mathcal{H}$  to  $h_n$ , from (2.19), is

$$\frac{1}{|\text{Aut}(\mathcal{H})|} \quad (3.3)$$

This maximum is, in fact, always saturated, for the following simple reason: one is free to twist any branch of a tree, without effecting the relative orientation of the other branches. In this way, one can untwist any twisted blob: all twists therefore contribute equally to the spherical average. We have demonstrated assertions (c) and (d) for single models, showing that the coefficient in  $h_n$  of any tree F-skeleton is precisely (3.2). Assertion (d) is just as true for multiple models as it is for single models. Assertion (c) holds as well, provided that one restricts oneself to trees with  $n$  edges in order  $n$ , because when  $\mathcal{H}$  has  $n$  edges,  $C_{\mathcal{G}}(\mathcal{H}, n) = C_{\mathcal{G}}(\mathcal{H})$  and the weight-entropy factor is one.

As has already been mentioned, all four assertions are substantiated by the third-order expansions for the free energy for the Potts model (2.17), the lattice (2.18), and multiple Ising models (2.20). The only F-skeletons which contribute to  $h_3$ , for instance, are the trees



and  $\begin{array}{c} \bullet \\ | \\ \bullet - \bullet - \bullet \end{array}$ . Their automorphism groups have order 2 and 6, respectively, which are the inverses of their coefficients for all three models.

#### 4. Counting trees

We have shown that  $h_n$ , the coefficient of  $\Delta^n$  in the  $n$ -th order term in the free energy, for any regular target graph describing a single model, is given by

$$h_n = \sum_{\mathcal{T} \in T_n} \frac{V(\mathcal{T})}{|\text{Aut}(\mathcal{T})|} \quad (4.1)$$

where  $T_n$  is the set of all unlabeled trees with  $n$  edges, and

$$V(\mathcal{T}) = \tilde{p}_1^{v_1} \tilde{p}_2^{v_2} \cdots \quad (4.2)$$

where  $v_k$  is the number of  $k$ -valent vertices in the tree  $\mathcal{T}$ . By putting  $a \rightarrow b = a\Delta$ , we expand  $F$  in inverse powers of  $\Delta$ :  $F = F_\infty + \mathcal{O}(\Delta^{-1})$ , where  $F_\infty = \sum_{n=1}^{\infty} h_n b^n$ . Given an unlabeled tree  $\mathcal{T}$  with  $n$  edges and  $n+1$  vertices, there are  $(n+1)!/|\text{Aut}(\mathcal{T})|$  distinct ways of labeling its vertices. Therefore,  $F_\infty$  can be expressed in a simpler way in terms of vertex-labeled trees:

$$F_\infty = \frac{1}{b} \sum_{n=2}^{\infty} \frac{b^n}{n!} \sum_{\mathcal{T} \in S_n} V(\mathcal{T}) \quad (4.3)$$

where  $S_n$  is the set of all vertex-labeled trees with  $n$  vertices (of which there are  $n^{n-2}$ , by Cayley's theorem). Once again:  $F_\infty$ —the free energy of the “universal model”—is independent of the target graph, and the same for any single model.

$F_\infty$  for multiple models can be expressed just as easily. First we derive it for  $\nu$  Ising models. A tree F-skeleton  $\mathcal{T}$  with  $m$  edges first appears in order  $b^m$ , and in every order thereafter. In  $m$ -th order, the coefficient of  $\mathcal{T}$  is as for a single model; in higher order  $n$  it is modified, as explained above. Specifically, two neighboring points in  $\mathcal{T}$  may have an edge in  $\mathcal{G}$  that is weighted  $a^2, a^3$ , etc. When coloring a new vertex in  $\mathcal{T}$  along an  $a^k$ -edge, there are  $\binom{\nu}{k}$  colors to choose from, as opposed to  $\nu$  colors for single models. Since we are interested in the leading term in  $\nu$ , we can approximate  $\binom{\nu}{k}$  by  $\nu^k/k!$ . The factors

$\nu^k$  combine to  $\nu^n$  in  $n$ -th order (see (2.3)). But there are different combinations of edge weights which give  $\nu^n$ : the sum is over all sets of  $m$  distinguishable positive integers whose sum is  $n$ , where each term is the inverse of the product of the factorials of the integers. The reader can work out a few examples for himself, but it is not hard to see that the extra factor in  $n$ -th order, besides the usual  $1/|\text{Aut}(\mathcal{T})|$  term, is just the coefficient of  $x^n$  in the Taylor expansion of  $(e^x - 1)^m$ , which is equal to

$$\frac{1}{n!} \sum_{k=0}^{m-1} (-1)^k \binom{m}{k} (m-k)^n. \quad (4.4)$$

One obtains the same sum by transforming the coupling constant  $b$  in (4.3)

$$b \rightarrow b' = e^b - 1 \quad (4.5)$$

Therefore, up to the transformation (4.5),  $F_\infty$  for multiple Ising models is equal to  $F_\infty$  for single models. Note that now  $F_\infty$  is the coefficient of the leading power of  $\nu$ . The above argument is easily generalizable to  $\nu$  copies of any single degree- $\Delta$  model; the transformation (4.5) becomes

$$b \rightarrow b' = e^{b\Delta} - 1. \quad (4.6)$$

The sum over trees  $\sum_{\mathcal{T} \in \mathcal{S}_n} V(\mathcal{T})$  has been expressed in an algebraic form by Riordan[11]. One defines the multi-variable Bell polynomials

$$Y_n(y_1, \dots, y_n) = e^{-y(x)} \left. \frac{d^n}{dx^n} e^{y(x)} \right|_{x=0}, \quad y(x) = \sum_{k=1}^{\infty} \frac{y_k}{k!} x^k. \quad (4.7)$$

Riordan then shows that

$$\sum_{\mathcal{T} \in \mathcal{S}_n} V(\mathcal{T}) = \tilde{p}_1^n Y_{n-2}(\theta \tilde{p}_2 \tilde{p}_1^{-1}, \dots, \theta \tilde{p}_{n-1} \tilde{p}_1^{-1}) \quad (4.8)$$

where—at the end of the calculation—one puts  $\theta^k \rightarrow (n)_k = n(n-1) \cdots (n-k+1)$ . For our purposes, this result can be re-expressed in a more convenient form by noticing that the Bell polynomial  $Y_n$  with the symbol  $\theta$  in every argument can be written

$$Y_n(\theta y_1, \dots, \theta y_n) = \left. \frac{\partial^n}{\partial x^n} [1 + y(x)]^n \right|_{x=0} \quad (4.9)$$



Therefore the sum over trees reduces to

$$\sum_{\mathcal{T} \in \mathcal{S}_n} V(\mathcal{T}) = \frac{\partial^{n-2}}{\partial \lambda^{n-2}} \left[ \frac{\partial \Pi}{\partial \lambda} \right]^n \Big|_{\lambda=0} \quad (4.10)$$

$$\Pi(\lambda, g) = \tilde{p}_1 \lambda + \frac{1}{2} \tilde{p}_2 \lambda^2 + \frac{1}{6} \tilde{p}_3 \lambda^3 + \dots$$

The vertex generating function  $\Pi(\lambda)$  is similar to the external field integral  $P(\Lambda)$  (which generates the twisted vertex factors  $p_{n,\tau}$ , see (2.10)), except that it does not discriminate the vertex factors according to twist. Therefore it is given by the much simpler scalar version of  $P(\Lambda)$ :

$$\Pi(\lambda, g) = \frac{1}{N^2} \log \frac{\int D\mu(\phi) e^{\sqrt{N} \lambda \text{Tr} \phi}}{\int D\mu(\phi)} \quad (4.11)$$

This may be calculated by the method of orthogonal polynomials, which gives

$$\Pi(\lambda, g) = \int_0^1 dx (1-x) \log \frac{r(x)}{x} - \frac{1}{N} \log \frac{h(g)}{h(0)} \quad (4.12)$$

where the function  $r$  satisfies the equations

$$\begin{aligned} -6gr &= -\lambda + s + 3gs^2 \\ -6g\lambda &= (1 + 6gs)(-\lambda + s + 3gs^2) \end{aligned} \quad (4.13)$$

and  $h(g) = \int_{-\infty}^{\infty} dx \exp \left[ \sqrt{N} \lambda x - V(x) \right]$ . In order  $\lambda^3$  and higher, the leading term in  $g$  in  $\Pi(\lambda, g)$  comes from the second term in (4.12), and in order  $\lambda^{n+2}$  is equal to

$$\frac{(2n)!}{n!(n+2)!} (3g)^n. \quad (4.14)$$

## 5. Discussion

We have shown that for regular target graphs of degree  $\Delta$  the leading term of the free energy in inverse powers of  $\Delta$ ,  $F_\infty$ , is identical (for single models) for all target graphs and contains contributions only from trees. In particular, after rescaling the matter coupling constant  $a \rightarrow b = a\Delta$ , the leading term is given simply by equation (4.3). This, after some combinatorial manipulations and simple observations concerning trees, can be shown to be equal to

$$F_\infty = \frac{1}{b} \sum_{n=2}^{\infty} \frac{b^n}{n!} \frac{\partial^{n-2}}{\partial \lambda^{n-2}} \left[ \frac{\partial \Pi}{\partial \lambda} \right]^n \Big|_{\lambda=0} \quad (5.1)$$

where  $\Pi(\lambda, g)$  is the one-matrix model average (4.11). An almost identical result holds for multiple models. For  $\nu$  copies of a model with target graph  $\mathcal{G}$  with degree  $\Delta$ , the leading term in the expansion of the free energy in inverse powers of  $\nu$  is identical to (5.1) after the transformations  $a \rightarrow b = a\nu$  and  $b \rightarrow b' = e^{b\Delta} - 1$ . These results have been shown to hold in every order of the low temperature expansion.

If  $\Delta$  becomes very large—and therefore the target graph becomes very large—we can ignore all but the leading term  $F_\infty$ . For the lattice and multiple 2, 3, or 4-state Potts models, this limit corresponds to central charge  $c \rightarrow \infty$ . The random surface picture is that of a series of “baby universes” (blobs) connected to each other as a tree (F-skeleton). The spins on each baby universe are frozen equal, while the spins on neighboring baby universes are unequal.

For ordinary multi-matrix models (on small target graphs), the cosmological constant  $g$  is coupled to the area of the surface, while the matter coupling constant  $a$  is coupled to the energy of the matter on the surface. The typical F-skeletons occurring in these models are highly multiply connected graphs. There are three critical regimes: adjusting  $g$  makes the area blow up; adjusting  $a$  orders the spins; and adjusting both yields a critical matter model on a continuous surface. For large target graphs, when we are left with the universal model which has only trees, the picture is different. The cosmological constant is still coupled to the *area*, but here this is the area of *each* baby universe. The matter coupling constant, however, is now coupled to the size (the number of edges, and therefore the number of vertices) of the tree. Adjusting  $g$  makes the areas of the baby universes blow up. Adjusting  $a$  makes the size of the tree—the number of baby universes—blow up. Finally, adjusting both yields an infinite tree whose vertices are continuous surfaces, the baby universes.

So one still gets a phase transition by adjusting the matter coupling constant, only it is a tree-growing—rather than a matter-ordering—transition. The matter coupling constant becomes a “second-quantized” cosmological constant. The critical exponent,  $\alpha$ , of the free energy is likely to be  $\frac{1}{2}$ . The reason is that if one puts the vertex factors  $\tilde{p}_n = 1$ , the sum over trees just reduces to the Cayley value  $n^{n-2}$  in  $n$ -th order; the coefficient of  $b^n$  grows as  $n^{n-2}/n! \approx n^{-5/2}e^n$ , which gives  $\alpha = \frac{1}{2}$ . The  $n^{-5/2}$  behavior is robust: it seems to be independent of the values of the vertex factors  $\tilde{p}_n$ ; we therefore expect that  $\alpha = \frac{1}{2}$ . It would be interesting to investigate the critical behavior of  $F_\infty$  systematically.

Interestingly,  $\frac{1}{2}$  is the value of the exponent found in [3] and [4], but for the “first-quantized” exponent  $\gamma_{\text{str}}$  rather than the “second-quantized” exponent  $\alpha$ . For a gaussian

model, of course, there is only one coupling constant and—generically—only one critical regime. Comparing our results with those of [3], we see that for the gaussian models one can blow up the trees, but not the baby universes. Perhaps this deviation from the universal model indicates a subtlety in the target space continuum limit.

Finally, we would like to point out the resemblance between our results and mean field theory. In ordinary spin models, the free energy becomes universal (i.e., independent of the type of matter) when the dimension of the *worldsheet* gets large. Here, the free energy for a two-dimensional worldsheet is universal when the dimension (or number of nearest neighbors) of the *target graph* is infinite. In ordinary spin models, the transition to universal, mean-field behavior occurs abruptly at a finite dimension. Could this also be the case for random surfaces?

### **Acknowledgements**

The author thanks Michael DeWeese, Alexander Migdal, Alan Sokal, and Joel Spencer for helpful discussions, and Edouard Brézin for the suggestion to study many Ising models.

## References

- [1] For an old but good review, see P. Ginsparg, “Matrix models of 2-d gravity,” Lectures given at Trieste Summer School, Trieste, Italy, July 22-25, 1991, hep-th/9112013.
- [2] M. Wexler, “Low temperature expansion of matrix models,” March 1993, Princeton preprint PUPT-1384, hep-th/9303146.
- [3] J. Ambjørn, B. Durhuus, J. Fröhlich and P. Orland, *Nucl. Phys.* **B270** [FS16] (1986) 457.
- [4] D.V. Boulatov, V.A. Kazakov, I.K. Kostov and A.A. Migdal, *Nucl. Phys.* **B275** [FS17] (1986) 641.
- [5] E. Brézin and S. Hikami, *Phys. Lett.* **283B** (1992) 203; *Phys. Lett.* **295B** (1992) 209.
- [6] I. Kostov, in *Non-perturbative aspects of the standard model: proceedings of the XIXth International Seminar on Theoretical Physics, Jaca Huesca, Spain, 6-11 June 1988*, eds. J. Abad, M. Belen Gavela, A. Gonzalez-Arrago (North-Holland, Amsterdam, 1989) 295.
- [7] D.J. Gross and M.J. Newman, *Phys. Lett.* **266B** (1991) 291.
- [8] E. Brézin, C. Itzykson, G. Parisi, and J.-B. Zuber, *Commun. Math. Phys.* **59** (1978) 35.
- [9] D. V. Boulatov and V. A. Kazakov, *Phys. Lett.* **186B** (1987) 379.
- [10] P. Erdős and A. Rényi, *Magyar Tudományos Akadémia Matematikai Kutató Intézetének Közleményei* **5** (1960) 17.
- [11] J. Riordan, *Bull. Amer. Math. Soc* **72** (1966) 110.